

Pronounced asymmetry in the crystallization behavior during constant heating and cooling of a bulk metallic glass-forming liquid

Jan Schroers,* Andreas Masuhr, and William L. Johnson

Keck Laboratory of Engineering Materials, California Institute of Technology, Pasadena, California 91125

Ralf Busch

Department of Mechanical Engineering, Oregon State University, Corvallis, Oregon 97331

(Received 22 July 1999)

The crystallization behavior of the supercooled bulk metallic glass-forming $Zr_{41}Ti_{14}Cu_{12}Ni_{10}Be_{23}$ liquid was studied with different heating and cooling rates. A rate of about 1 K/s is sufficient to suppress crystallization of the melt upon cooling from the equilibrium liquid. Upon heating, in contrast, a rate of about 200 K/s is necessary to avoid crystallization. The difference between the critical heating and cooling rate is discussed with respect to diffusion-limited growth taking classical nucleation into account. The calculated asymmetry of the critical heating and cooling rate can be explained by the fact that nuclei formed during cooling and heating are exposed to different growth rates. [S0163-1829(99)07441-X]

The ability to form a glass by cooling from the equilibrium liquid is equivalent to suppressing crystallization within the supercooled (undercooled) liquid. One of the central quantities in theoretical and experimental studies of glass formation is the critical cooling rate R_c to bypass crystallization upon cooling from the stable melt.¹ Critical cooling rates of monoatomic metallic systems are typically of the order of 10^{12} K/s. In contrast, R_c of recently discovered multicomponent bulk metallic glass-forming alloys^{2,3} is of the order of a few K/s. This excellent glass-forming ability enables investigations of crystallization,^{4,5} viscosity,⁶ and diffusion^{7,8} as well as relaxation⁹ in the supercooled liquid region. The critical cooling rate of $Zr_{41}Ti_{14}Cu_{12}Ni_{10}Be_{23}$ (Vit 1), studied in this work, is about 1 K/s.¹⁰ In contrast, crystallization of amorphous Vit 1, previously investigated by differential scanning calorimetry (DSC) upon heating¹¹ could not be avoided up to the maximum heating rate of the DSC of 5 K/s and the critical heating rate has not been determined yet. The critical heating rate R_h , the counterpart of the critical cooling rate upon heating, is the lowest rate an amorphous sample can be heated through the entire supercooled liquid region without crystallization.

In this paper, the onset temperature of crystallization is investigated during cooling from the stable melt and heating amorphous Vit 1 as a function of cooling and heating rate, respectively. For this purpose we designed an experimental setup that permits maximum heating rates of 350 K/s and maximum cooling rates of 40 K/s. We will show that an asymmetry of R_c and R_h results from the fact that nuclei formed during cooling and heating are exposed to different growth rates, which is likely to be a general feature for metallic systems.

The investigations were performed in high-purity graphite crucibles since heterogeneous surface nucleation at the container walls does not effect the crystallization of the bulk Vit 1 sample.¹² The samples were mounted into the graphite crucibles and inductively heated in vacuum of 10^{-6} mbar or in a titanium-gettered argon atmosphere. The temperature was

measured using a thermocouple (type K) with an accuracy better than ± 2 K. Details of the experimental setup can be found elsewhere.¹³

Amorphous and crystalline Vit 1 samples were heated with rates between 0.6 and 200 K/s. The digitally recorded temperature-time profiles were differentiated and are plotted versus temperature in Fig. 1. Prior to each heating procedure, the sample was heated to 1175 K and subsequently cooled to room temperature with a rate of 5 K/s, which resulted in the formation of an amorphous sample. Crystalline samples were prepared by cooling from 1175 K with a rate of 0.2 K/s. The crystallization of the melt in a heating experiment is detected by a temperature rise, so-called recalescence, which has its origin in the release of the heat of fusion at the solid/liquid interface during crystallization. The recalescence leads to an increase of the heating rate. The onset of recalescence is marked by arrows in Fig. 1. With increasing heating rate the crystallization temperatures shifted to higher temperatures.

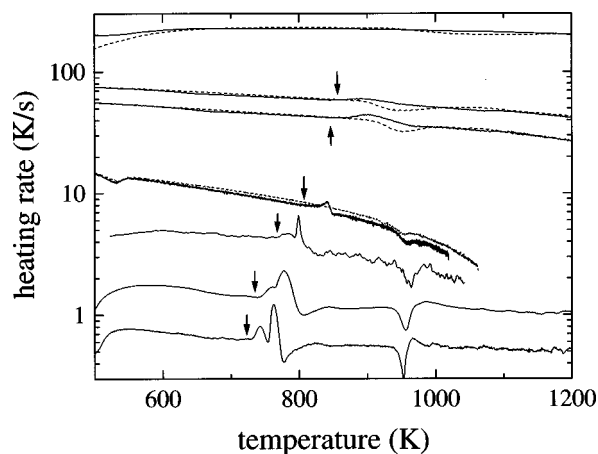


FIG. 1. Derivative of the temperature-time profile, recorded during heating of amorphous (solid line) and crystalline (dashed line) Vit 1, vs temperature. The onset of recalescence is marked by arrows.

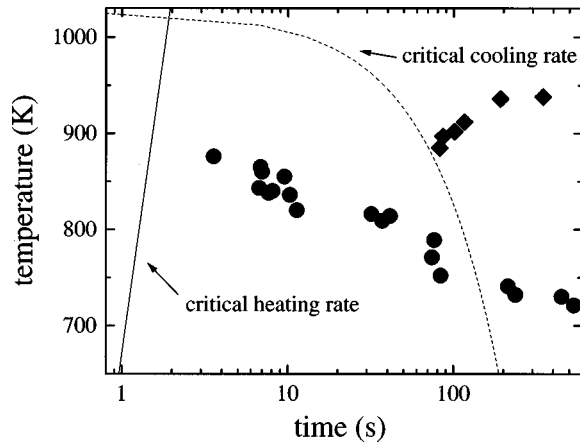


FIG. 2. Continuous cooling and heating diagram of Vit 1. In this diagram the cumulative time during constant heating and cooling from the glass transition temperature and the equilibrium liquid, respectively, is plotted versus temperature. Diamonds (◆) denote the onset of crystallization for samples cooled from the equilibrium melt. The onset of crystallization for samples heated from the amorphous state is shown by circles (●). The critical cooling rate of about 1 K/s and the critical heating rate of approximately 200 K/s are denoted by the dashed and solid lines, respectively.

No crystallization was observed upon heating amorphous Vit 1 with a rate of 200 K/s. In contrast, melting could still be detected during heating crystalline Vit 1 with the same rate. At this high heating rate, the amorphous sample is heated through the entire supercooled liquid regime from the glass transition temperature into the equilibrium melt without a detectable crystallization event.

The continuous heating and cooling diagram for Vit 1 is shown in Fig. 2. In this diagram the cumulative time until crystallization is detected during constant heating from the glass transition temperature and cooling from the equilibrium liquid is plotted versus temperature. This diagram reveals a large asymmetry in the crystallization behavior between cooling from the stable melt and heating the amorphous sample. In agreement with previous results¹⁰ we found a critical cooling rate for Vit 1 of about 1 K/s. However, the critical heating rate of approximately 200 K/s is about two orders of magnitude larger. A difference in crystallization behavior between cooling from the stable melt and heating the amorphous sample was also suggested for the Ni₄₀Pd₄₀P₂₀ bulk metallic glass-forming system.¹⁴

In an experiment, the onset of crystallization is somewhat arbitrarily defined as the point in time where the crystalline volume fraction within the melt reaches some small but finite value. With the present setup a crystallized volume fraction of about 10^{-3} can be detected. The exact value of the detectable volume fraction has, however, marginal influence on the present discussion. Crystallization of a melt requires the formation of nuclei and subsequent growth of crystalline phases. Within classical nucleation theory, the steady state nucleation rate

$$I_{SS} = AD \exp\left[-\frac{\Delta G^*}{kT}\right] \quad (1)$$

is the product of a constant A , an effective diffusivity D , and the thermodynamic Boltzmann factor to overcome the nucle-

ation barrier. T denotes the absolute temperature, and k is Boltzmann's constant. In a complex system like Vit 1 an adequate description of the nucleation process will certainly have to go beyond the concept of steady-state nucleation.⁵ Further influences such as, for example, decomposition processes, have to be considered¹⁵⁻¹⁷ to explain the fine microstructures of Vit 1.⁵ At this point, however, to discuss the different growth kinetics on crystallization the simplified approach of steady-state nucleation serves as a sufficient model.

The activation energy to form a critical nucleus is given by $\Delta G^* = 16\pi/3 \times \sigma^3 / \Delta G^2$. Here σ denotes the energy of the interface between the melt and a nucleus and ΔG the difference in Gibbs free energy between the solid and liquid phases. Assuming diffusion-limited growth, the crystalline growth velocity can be described by

$$u = \frac{D}{a} \left[1 - \exp\left(-\frac{\Delta G}{kT}\right) \right], \quad (2)$$

with the interatomic spacing a . The temperature dependence of the effective diffusivity is described by a hybrid equation that was proposed earlier.⁶ The interfacial energy $\sigma = 0.04$ J/m² and $A = 10^{11.1}$ were taken from a least-squares fit to the isothermal temperature-time-transformation (TTT) diagram.⁶ DSC results from Ref. 11 were taken as an estimate for ΔG . Considering three-dimensional growth and a steady-state nucleation rate, the time-dependent volume fraction x of crystallized material is obtained by

$$x(t) = \frac{4\pi}{3} \int_0^t I(T, \tau) \left[\int_\tau^t u(T, T') dt' \right]^3 d\tau. \quad (3)$$

The double integral sums over all nucleation centers appearing at time τ and their growth from τ to time t . The crystallized volume fraction [Eq. (3)] is numerically calculated for linear cooling and heating and plotted versus temperature in Fig. 3. x increases continuously upon cooling from the liquidus temperature T_{liq} with 1 K/s and becomes approximately constant at 600 K [curve (a) in Fig. 3]. The calculation was terminated at 500 K due to the freezing of the crystallization kinetics. The total crystallite volume fraction of 3.5×10^{-4} would not be observed in the thermocouple signal of the present experimental setup. Continuing the simulation by heating the sample with the same rate of 1 K/s leads to the detection of the onset of crystallization ($x = 1 \times 10^{-3}$) at 820 K [curve (b) in Fig. 3]. For comparison, a simulation with a perfectly amorphous sample, heated with 1 K/s, is also shown in Fig. 3 [curve (c)]. Here the crystallization becomes detectable at 880 K.

For steady-state nucleation, the number of nuclei formed during heating of a perfectly amorphous sample up to the liquidus temperature is exactly the same as the number of nuclei formed during cooling from T_{liq} down to the glass transition temperature T_g . However, the nuclei formed during cooling are exposed to different growth rates than nuclei formed during heating. The nucleation rate and growth rate according to Eqs. (1) and (2), respectively, were calculated

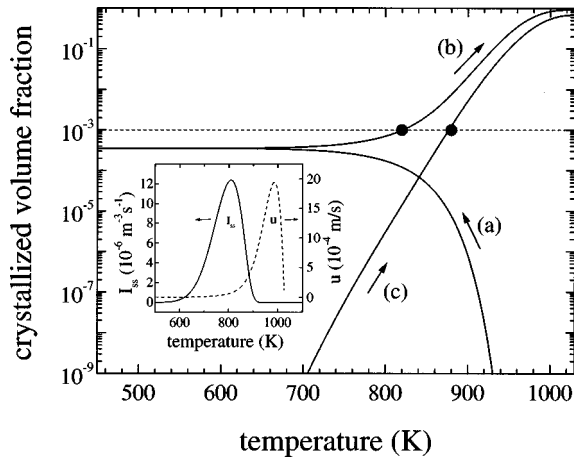


FIG. 3. Calculated crystallized volume fraction according to Eq. (3), for linear heating and cooling of Vit 1. Cooling from the equilibrium melt (a) with 1 K/s results in a volume fraction of crystallized material of 3.5×10^{-4} . Reheating this sample with 1 K/s (b) leads to the detection of the onset of the recalcination at 820 K. For heating a perfectly amorphous sample with 1 K/s (c) crystallization becomes detectable at 880 K. The inset shows the nucleation rate I_{ss} (solid line) and growth rate u (dashed line) calculated with the above-mentioned parameters (Ref. 13), according to Eqs. (1) and (2), respectively.

with the above-mentioned parameters. The maximum of the growth rate at 985 K is at a much higher temperature than the maximum of the nucleation rate at 840 K (inset in Fig. 3). Therefore, upon heating a perfectly amorphous sample, a large number of nuclei have formed at the temperature where the nucleation rate has a maximum. During further heating, these nuclei are exposed to the maximum growth rate, resulting in a high crystallization rate. In contrast, upon cooling from T_{liq} , the maximum number of nuclei formed at the same temperature will experience lower growth rates during further cooling to T_g , leading to a low crystallization rate. The result is that a higher volume fraction of crystallites formed during heating of a perfectly amorphous sample, compared to the one crystallized upon cooling with the same rate from T_{liq} . If the effect of quenched-in nuclei is taken into account, the difference is even larger. Consequently, to keep x below the detection level, the sample has to be heated faster from the amorphous state than cooled from the equilibrium liquid. The calculations yield $R_c = 1$ K/s and $R_h = 9$ K/s. This suggests that the effect that nuclei formed during cooling and heating are exposed to different growth rates to a great extent accounts for the experimental finding of a large difference between R_c and R_h . Further contributing factors which have to be considered may be the following.

(i) Since the critical nucleus size decreases with undercooling, not only overcritical clusters (nuclei) are quenched in upon cooling, but also undercritical clusters. These undercritical clusters become overcritical at lower temperatures. During reheating, their subsequent growth additionally contributes to the crystallization process, leading to an even stronger asymmetry between the critical cooling and the critical heating rate.

(ii) There are indications in the Vit 1 system for a chemical decomposition process within the undercooled melt.^{15,16,4} These concentration modulations partially shift the composi-

tion towards the composition of the primarily solidified phase, which causes an increase of the nucleation probability. The resulting high nucleation rate would also lead to a faster crystallization process upon reheating.

Both factors would lower the position of the maximum in the nucleation rate and enhance the asymmetry of R_c and R_h .

At this point the question arises whether our experimental findings should in general be found in metallic liquids or, if under certain conditions, the asymmetry vanishes or is even reversed. This would be the case if the maximum of the nucleation rate was found above the maximum of the growth rate. The interfacial energy is one parameter that strongly affects the location of the maximum of nucleation and the growth rate. Therefore, the interfacial energy was varied in our simulation. The location of the maximum in nucleation and the growth rate could be brought to a match if an interfacial energy of 5×10^{-5} J/m² was assumed. This interfacial energy is three orders of magnitude smaller than the value of 0.04 J/m², obtained from the fit to the experimental TTT diagram. The interfacial energy is directly related to the entropy of fusion. Since all metals and alloys show heats of fusions that are not far away from $\Delta S \approx 8.3$ J/g atom K, given by Richard's rule, the interfacial energies in supercooled liquids for moderate undercooling (far about the isentropic temperature) are always of the order of 10^{-1} J/m². Thus the assumption of much smaller values is physically not reasonable.

The diffusivity in the supercooled liquid affects the maximum in growth as well as the maximum in nucleation rate. The diffusivity is assumed to follow a hybrid equation as mentioned above. At high temperatures the diffusivity is inversely proportional to the viscosity. Vit 1 is a relatively "strong" liquid,¹⁸ which means it exhibits a large viscosity around the melting point of 2.5 Pa s and a large apparent activation energy of 2.0 eV for flow.⁶ This contrasts with most pure metals and alloys, which are considered "fragile" liquids with much lower viscosities at the melting point of 10^{-3} Pa s and an apparent activation energy of 0.5 eV.¹⁹ Thus, in general, the kinetics in other metallic systems is much faster than in Vit 1, resulting in rapid crystallization. We investigated if in such a metallic system the maximum in the growth rate can be lowered in a way that it reduces or eliminates the observed asymmetry. If we assume a fragile liquid, the maximum in growth rate decreases. However, the maximum in nucleation rate is also shifted to lower temperatures. Therefore, even in pure metals the asymmetry between heating and cooling should be observed since no crossover occurs. In other words, the present investigation shows more generally that, if any metallic liquid is quenched and forms an amorphous solid, it has to be heated even faster to retain its noncrystalline state.

In conclusion, linear heating and cooling experiments were performed on Vit 1 samples and a constant heating and cooling diagram was determined. Cooling Vit 1 from the equilibrium melt requires a rate of about 1 K/s to suppress crystallization. In contrast, crystallization could only be avoided upon heating amorphous Vit 1 with a rate as high as 200 K/s. The effect that nuclei, formed during cooling and heating, are exposed to different growth rates to a great ex-

tent accounts for the experimental finding of a large difference between critical cooling and heating rate. However, the observed microstructures⁵ are much finer than would be expected after steady-state nucleation. This suggests that contributions such as phase separation and quenched-in under-

critical clusters further contribute to the large asymmetry between the measured critical cooling and critical heating rate.

This work was supported by the National Aeronautics and Space Administration (Grant No. NCC8-119) and the Department of Energy (Grant No. DEFG-03086ER45242).

*Electronic address: schroers@hyperfine.caltech.edu

¹P. G. Debenedetti, *Metastable Liquids* (Princeton University Press, Princeton, 1996).

²A. Inoue, T. Zhang, and T. Masumoto, *Mater. Trans., JIM* **31**, 177 (1990).

³A. Peker and W. L. Johnson, *Appl. Phys. Lett.* **63**, 2324 (1993).

⁴W.-H. Wang, Q. Wei, S. Friedrich, M. P. Macht, N. Wanderka, and H. Wollenberger, *Appl. Phys. Lett.* **71**, 1053 (1997); W.-H. Wang, Q. Wei, and S. Friedrich, *Phys. Rev. B* **57**, 8211 (1998).

⁵J. Schroers, R. Busch, A. Masuhr, and W. L. Johnson, *Appl. Phys. Lett.* **74**, 2806 (1999).

⁶A. Masuhr, T. A. Waniuk, R. Busch, and W. L. Johnson, *Phys. Rev. Lett.* **82**, 2290 (1999).

⁷U. Geyer, S. Schneider, W. L. Johnson, Y. Qui, T. A. Tombrello, and M.-P. Macht, *Phys. Rev. Lett.* **75**, 2364 (1995).

⁸H. Ehmler, A. Heesemann, K. Rätzke, F. Faupel, and U. Geyer, *Phys. Rev. Lett.* **80**, 4919 (1998).

⁹A. Meyer, J. Wuttke, W. Petry, O. G. Randl, and H. Schober, *Phys. Rev. Lett.* **80**, 4454 (1998).

¹⁰Y. J. Kim, R. Busch, W. L. Johnson, A. J. Rulison, and W. K. Rhim, *Appl. Phys. Lett.* **65**, 2136 (1994).

¹¹R. Busch, Y. J. Kim, and W. L. Johnson, *J. Appl. Phys.* **77**, 4039 (1995).

¹²A. Masuhr, R. Busch, and W. L. Johnson, *Mater. Sci. Forum* **269-272**, 779 (1998).

¹³A. Masuhr, Ph.D. thesis, California Institute of Technology, 1999.

¹⁴H. W. Kui and D. Turnbull, *Appl. Phys. Lett.* **47**, 796 (1985).

¹⁵R. Busch, S. Schneider, A. Peker, and W. L. Johnson, *Appl. Phys. Lett.* **68**, 493 (1996).

¹⁶S. Schneider, P. Thiyagarajan, and W. L. Johnson, *Appl. Phys. Lett.* **68**, 493 (1995).

¹⁷K. F. Kelton, *Philos. Mag. Lett.* **77**, 337 (1997).

¹⁸R. Busch, A. Masuhr, E. Bakke, and W. L. Johnson, *Mater. Sci. Forum* **269-272**, 547 (1998).

¹⁹T. Iida and R. I. L. Guthrie, *The Physical Properties of Liquid Metals* (Clarendon, Oxford, 1988).